

Photoluminescence processes in Si_mGe_n superlattices

Subhasis Ghosh* and Jörg Weber†

Max-Planck-Institut für Festkörperforschung, Postfach 80 06 65, D-70506 Stuttgart, Germany

Hartmut Presting

Daimler-Benz Research Centre, Postfach 2360, 89013 Ulm, Germany

(Received 14 February 2000)

We have studied at low temperatures the near band-edge photoluminescence in Si_mGe_n strained layer superlattices grown by molecular-beam epitaxy on step-graded alloy buffers. The excitation density dependence and the time decay of the photoluminescence identify the origin of the no-phonon transitions in Si_6Ge_4 and Si_9Ge_6 strained layer superlattices. At high excitation powers, recombination due to localized excitons dominates, whereas at low excitation powers a faster decay of bound excitons localized to impurities prevails.

I. INTRODUCTION

The growth and properties of Si_mGe_n strained layer superlattices (SLS) on Si has attracted intense interest, not only because of the technological prospects of band-gap engineering and possible Si-based optoelectronic devices, but also due to the physics of pseudodirect band-gap systems.¹ The tremendous progress in the growth of high quality strained epitaxial layers by molecular-beam epitaxy led recently to convincing evidence for a pseudodirect band gap in Si_mGe_n SLS.²⁻⁵ In particular, the drastic reduction of the dislocation density by step-graded buffer layers and the sharp interfaces generated by the surfactant technique were crucial for an enhanced light emission in the near-infrared region. The interband optical transition in Si_mGe_n SLS was interpreted as a direct transition between the new minibands created by zone folding.^{6,7} The experimental observations led to many theoretical studies, which showed that a quasidirect band gap can be realized in Si_mGe_n SLS, if the Si layers are under tensile strain.⁷⁻¹⁰ Experimentally, this was realized by growing a Si_mGe_n SLS on a relaxed $\text{Si}_x\text{Ge}_{1-x}$ buffer layer. Some controversy existed regarding the origin of the intense photoluminescence (PL) peak in earlier Si_6Ge_4 SLS samples that usually contained high dislocation densities.³ Nowadays, it is possible to grow high quality samples with a low dislocation density on completely relaxed alloy buffers with step-graded Ge concentration. The pronounced increase in the PL intensity at the same transition energy in samples with low dislocation densities is a clear argument against the suggestion that the PL originates from dislocations in the Si_mGe_n SLS.^{11,12} Until recently, little was known about the optical properties of the SLS, but the discovery of well-resolved near band-gap transitions makes PL a standard technique to characterize and study the optical properties of Si_mGe_n SLS structures.^{3,4} One of the contentious issues regarding the PL processes involves the origin of band-edge recombination processes. In relaxed, bulk SiGe alloys, well-resolved free exciton (FE), bound exciton (BE), and also excitons trapped by random potential fluctuations, known as localized excitons (LE), were reported.¹³ The localized excitons were extensively studied in other alloy semiconductors.^{14,15} Lenchy-

shyn and co-workers observed photoluminescence from BE and LE in $\text{Si}_x\text{Ge}_{1-x}$ epitaxial layers.¹⁶ Band-edge transitions that were related to LE and BE (or FE) recombination were also reported in Si- $\text{Si}_x\text{Ge}_{1-x}$ -Si thin quantum wells.¹⁷ Menczgar *et al.*, have observed similar band-edge no-phonon (NP) transitions in Si_mGe_n SLS and from a line-shape analysis they attributed the optical transition to a LE recombination.⁴ However, a detailed analysis of the possible recombination processes is still missing. In the present paper, we study in detail the mechanism of PL processes at various excitation conditions in two Si_mGe_n SLS. Depending on the excitation power, two distinct types of spectra are observed. Under high excitation conditions the characteristic LE line shape due to the exponential density-of-states is detected. At low excitation powers the line shape is in agreement with a BE recombination. A range of excitation intensities exists where one observes a superposition of both BE and LE spectra. The excitation power dependence of the PL spectra along with the time decay of the PL confirm the two different recombination processes.

II. EXPERIMENTAL DETAILS

The Si_mGe_n SLS structures were grown on a buffer layer in a Si-MBE system. The SLS structures contain six monolayers of Si followed by four monolayers of Ge (Si_6Ge_4) or nine monolayers of Si followed by six monolayers of Ge (Si_9Ge_6). The buffer layer consists of an 100-nm Si layer grown at 600 °C, followed by a step-graded alloy $\text{Si}_{1-y(z)}\text{Ge}_{y(z)}$ layer with a thickness of 650 nm. The Ge content in the step-graded buffer layer was varied stepwise with $\Delta y/d = 3\%/50$ nm, the growth temperature was decreased from 600 °C to 520 °C. Finally, ontop of the step-graded buffer layer a 500 nm thick $\text{Si}_{0.6}\text{Ge}_{0.4}$ alloy layer follows, which was grown at 520 °C. The superlattice structure consists of 110 periods with an entire thickness of roughly 150 nm for Si_6Ge_4 and 100 periods with a thickness of roughly 215 nm for Si_9Ge_6 . A monolayer of Sb was deposited on the buffer layer as surfactant before the growth of the superlattice to enhance the sharpness of the interface. The Si_mGe_n SLS structures were characterized by cross-sectional

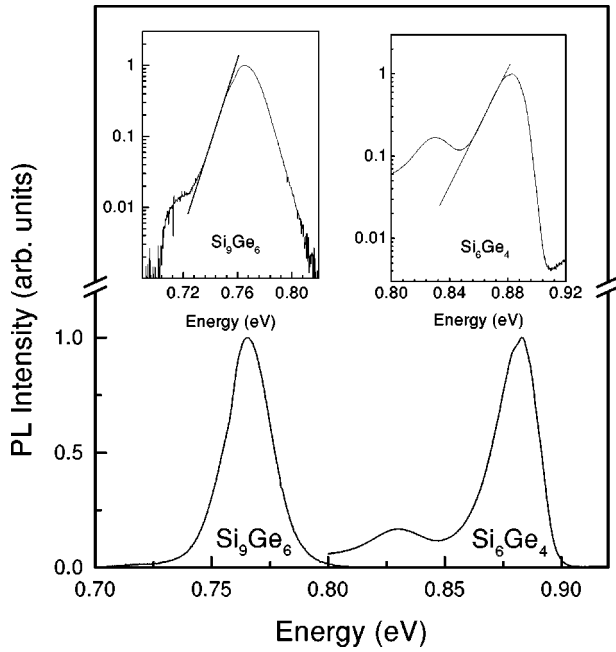


FIG. 1. PL spectra of Si_6Ge_4 and Si_9Ge_6 SLS under identical excitation conditions (laser power = 100 mW cm^{-2} , $T = 1.8 \text{ K}$, and $\lambda_{exc.} = 457 \text{ nm}$). The inset shows the semilog plot of the same PL spectra. The low-energy edge of the NP peaks are fitted with straight lines indicating an exponential dependence.

transmission electron microscopy (TEM), x-ray diffraction (XRD), and Raman scattering. The dislocation density was determined by cross-sectional TEM. The period length of the superlattice structures was determined with TEM and XRD.

The samples were immersed in liquid helium at 4.2 K or at 1.8 K in an optical cryostat. Front surface excitation by the 457- or 514-nm lines of an Ar^+ ion laser was used. The excitation density could be varied from $10 \mu\text{W cm}^{-2}$ to 1 W cm^{-2} . The penetration depth of the laser light in the sample varied from $0.27 \mu\text{m}$ at 457 nm to $2.7 \mu\text{m}$ at 514 nm. An infrared filter was used to block all light shorter than 1000 nm. The PL signal in the wavelength region of 1000–1800 nm was dispersed by a 1 m grating monochromator and detected with a liquid-nitrogen-cooled Ge detector. The detector signal was amplified in lock-in technique. The spectral response of the system was calibrated to a black body source. The PL time decay was determined by pulsing the laser with an acousto-optic modulator. The PL signal was detected by a fast photodetector with 5 ns risetime and a transient recorder. The time resolution in the whole setup was of the order of 10 ns.

III. EXPERIMENTAL RESULTS

A. General features of the photoluminescence spectra

Figure 1 presents the near band-edge PL spectra of two SLS samples (Si_6Ge_4 and Si_9Ge_6). The excitation density was $\sim 100 \text{ mW cm}^{-2}$. The NP transitions are centered at 0.882 eV in Si_6Ge_4 and 0.765 eV in Si_9Ge_6 . The NP peaks shift as expected towards higher energies with decreasing number of Ge monolayers. The transition energies as a function of period length ($m+n=10$, $m+n=15$) match well the results from effective-mass calculations.^{3,4,7} The addi-

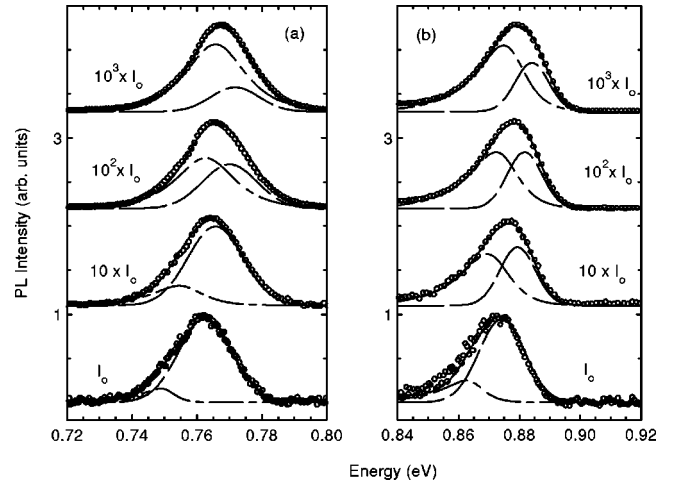


FIG. 2. Low temperature (1.8 K) PL spectra of a Si_9Ge_6 SLS (a) and a Si_6Ge_4 SLS (b) for four different excitation conditions with $I_0 \sim 0.1 \text{ mW cm}^{-2}$. Empty circles represent the experimental data. The experimental line shape was fitted by two recombination processes: A Gaussian line (shown by the bigger dash) for the high-energy component and an LE line shape (shown by smaller dash) for the low-energy component. All spectra are scaled to show the relative intensities of the two NP components.

tional PL signals shown in Fig. 1 detected at 0.831 eV in Si_6Ge_4 SLS and 0.715 eV in Si_9Ge_6 SLS are due to momentum-conserving phonon replicas involving $\text{TO}_{\text{Si-Ge}}$ phonons. Similar PL spectra for samples from the same wafers have been reported in Ref. 4 and it has been shown that the origin of the near band-edge PL and dislocation related defect lines is different by annealing the SLS structures at high temperatures. In annealed (600°C) Si_6Ge_4 SLS the near band-edge PL lines shift to higher energies due to the interdiffusion of the layers.¹⁸ Further annealing of the sample at 780°C results in dislocation related D_1 and D_2 lines.

The insets of Fig. 1 show a semilog plot of the same PL spectra. The line shape of the NP peaks evolves from the recombination of excitons trapped at localized sites in the band tails. The lower energy side varies as $\exp(E/E_0)$ with $E_0 = 11.5 \text{ meV}$ in Si_6Ge_4 and $E_0 = 8.5 \text{ meV}$ in Si_9Ge_6 . The same values for E_0 are derived from the spectral analysis of the phonon replicas.

B. Variation with excitation power

The NP peaks are found to be a composition of a low-energy and a high-energy component. Differences in the excitation dependence allow a separation of the two components. Figure 2 shows PL spectra under four different excitation densities. A shift of the NP peak with excitation and small changes in the line shape are visible. We were able to model the changes in peak position and line shape with excitation density by using different intensities of the two components. At low excitation ($I_0 \sim 0.1 \text{ mW cm}^{-2}$) the spectra are dominated by the high-energy component; high excitation densities ($10^3 \times I_0$) are favorable for the low-energy component. The high-energy component is fitted by a Gaussian line shape and the low-energy component by the typical LE line shape that is given in Ref. 15,

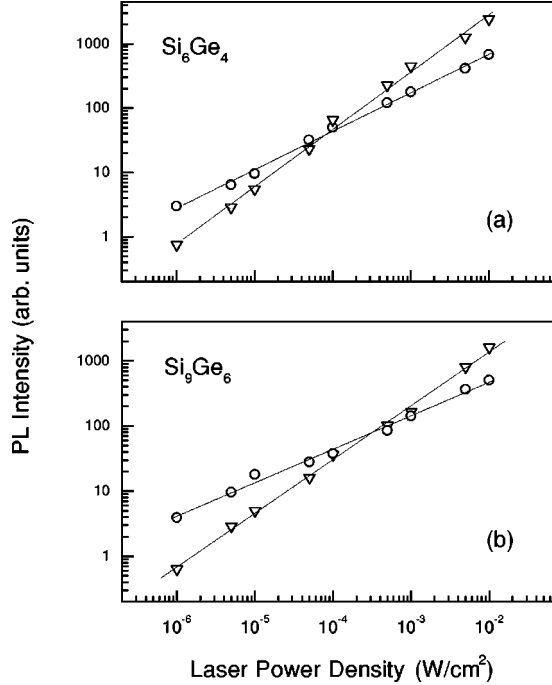


FIG. 3. Dependence of the integrated PL intensity on excitation power for the low-energy (∇) and high-energy (\circ) components. (a) Si_6Ge_4 SLS and (b) Si_9Ge_6 SLS.

$$I(E) \propto \exp(E/E_0) \left[\frac{1}{\tau_{rad}} + \gamma \exp\left(\frac{E_c - E}{k_B T}\right) \right]^{-1}. \quad (1)$$

The first factor $\exp(E/E_0)$ originates from the density-of-states due to potential fluctuations in the SLS and the second term describes the radiative recombination efficiency of LE. E_c is the mobility edge of the energy states and the high-energy cutoff for the PL spectra. τ_{rad} is the radiative life time of LE and γ is the effective frequency for thermal excitation attempts. τ_{rad} is determined experimentally, which will be described in the next section. We remark that the high-energy peak can also be fitted by a Lorentzian line shape, but it was found that the Gaussian line shape gives the best results. A similar deconvolution (not shown) of the phonon replicas gives the same dependence. The ratio of the NP/TO PL intensity for both, the low-energy and the high-energy component does not depend on the excitation density. The low-energy component lies 9 meV below the high-energy component in Si_6Ge_4 and 12 meV in Si_9Ge_6 . This separation depends weakly on the excitation intensity. The position of the separate components as well as the superposed NP peak, shift slightly towards higher energies with excitation densities, due to the increased screening of the potential fluctuations.

The excitation dependence of the PL spectra for Si_6Ge_4 and Si_9Ge_6 SLS is shown in more detail in Fig. 3. The NP components increase following the relation $I \propto P^m$, where I is the integrated PL intensity and P is the laser power density. The high-energy component shows a sublinear dependence of $m=0.59$ for Si_6Ge_4 and $m=0.52$ for Si_9Ge_6 . The low-energy NP peak shows almost linear dependence with $m=0.9$ for Si_6Ge_4 and $m=0.82$ for Si_9Ge_6 . A sublinear power dependence is a typical behavior for BE recombination processes. An increasing number of electron-hole pairs

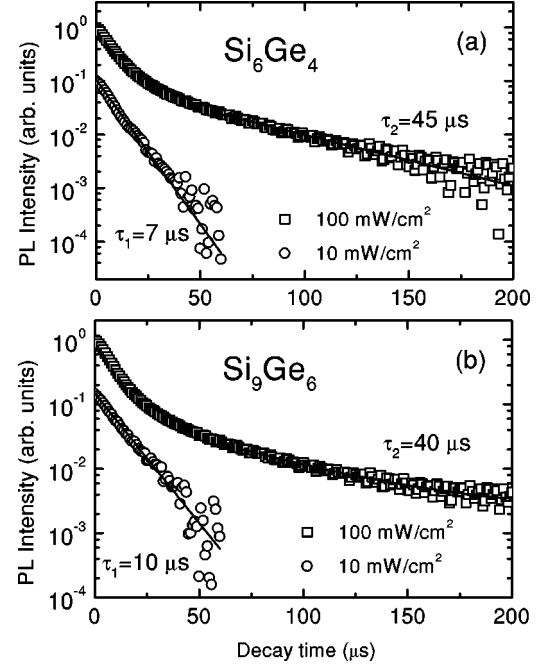


FIG. 4. Time decay of the PL from (a) Si_6Ge_4 and (b) Si_9Ge_6 SLS. The PL decay at lower excitation intensities (I_0) is exponential. As the excitation power is increased ($10^1 \times I_0$) another slow component appears and the PL decay becomes biexponential.

leads to a saturation of BE complexes, due to the finite number of impurities. Recombination of the excitons via potential fluctuations (LE) with a linear power dependence is always possible and the preferred transition at high excitation powers.

C. Time-resolved photoluminescence

Further support for the two NP components in the PL spectra comes from time-resolved photoluminescence measurements. In Fig. 4 the PL decay curves for the Si_6Ge_4 and Si_9Ge_6 samples are given. At low excitation the PL decreases with a single exponent. As the excitation power increases another slow component appears and the whole decay can be fitted with a biexponential function

$$I = A \exp(-t/\tau_1) + B \exp(-t/\tau_2). \quad (2)$$

The spectral resolution of the time-resolved measurements is poor, due to the weak intensity of the luminescence. Therefore, the time decay of the high- and the low-energy component cannot be determined separately. However, the intensity dependence of the time decay suggests that τ_1 and τ_2 are the lifetimes of the high-energy component and the low-energy component, respectively. We determine $\tau_1 = 7 \mu\text{s}$ in Si_6Ge_4 and $10 \mu\text{s}$ in Si_9Ge_6 and $\tau_2 = 45 \mu\text{s}$ in Si_6Ge_4 and $40 \mu\text{s}$ in Si_9Ge_6 . The intensity of the slow decay increases with excitation intensity and the intensity of the fast decay saturates, which is consistent with the excitation density dependent PL spectra shown in Fig. 2. A similar biexponential PL decay was already observed in GaAs/AlAs short period superlattices, there the slower decay was also identified with the recombination of localized excitons.¹⁹

IV. DISCUSSION

The behavior of the two NP transitions in Si_mGe_n SLS is very similar to the near band-gap luminescence in bulk Si-Ge layers.¹³ In these layers a high-energy and a low-energy component was assigned to BE and LE recombinations, respectively. In low dimensional Si-Ge systems a high-energy NP component was identified and assigned to BE recombinations.^{16,17} In the presence of impurities and potential fluctuations, it seems to be unlikely that a FE recombination exists at low temperatures ($T \leq 4.2$ K). The quantum efficiency of the BE recombination at low temperature is maximum among all possible recombination processes in direct gap as well as in indirect band-gap semiconductors. In the case of Si, even for very low concentrations of shallow dopants ($\sim 10^{13} \text{ cm}^{-3}$), the BE transitions dominate the PL spectra.

In Si_mGe_n SLS structures an exponential low-energy tail was already reported for the near band-gap luminescence.⁴ Our experimental results confirm the typical LE line shape that reflects the density-of-states. In addition, we find a dominance of the low-energy component at high excitation power, a linear dependence of the PL intensity on excitation power, and a long radiative lifetime ($\sim 40\text{--}50 \mu\text{s}$). All our results clearly identify the low-energy component as due to a recombination of LE.

The high-energy component shows a dominance at low excitation powers, a Gaussian line shape, a sublinear dependence of the PL intensity on excitation power, and a faster radiative lifetime ($\sim 7\text{--}10 \mu\text{s}$). All these properties are characteristic of BE recombination.

The energy separation between LE and BE increases with Ge layer thickness in the Si_mGe_n SLS from 9 meV in Si_6Ge_4

to 12 meV in Si_9Ge_6 . In the case of Si_mGe_n SLS, electrons are confined in the Si layers and holes in Ge layers, because of the type-II band alignment. As the thickness of the Ge layer decreases, the excitons are constrained to move in two dimensions rather than three dimensions and the probability of exciton hopping and/or tunneling to the deeper states of the fluctuating potential becomes reduced. Similar explanations were given in Si-SiGe-Si quantum wells¹⁷ and GaAs-GaSb-GaAs²⁰ superlattices. Moreover, the binding energy of the excitons also depends on the symmetry of the wave function. With decreasing well thickness the ground-state wave function of the exciton becomes p type and the binding energy becomes almost half of that of an s -type wave function. At present, it is not possible to specify which mechanism is more effective for the variation of LE binding energy.

V. SUMMARY

In this paper we presented a study of the strong near band-edge PL transitions in Si_mGe_n SLS with different period lengths. Two different excitonic transitions contribute to the NP band-edge PL. From the excitation power dependence of the PL spectra and time-resolved PL, we attribute the low-energy component to a LE recombination and the high-energy component to a BE recombination.

ACKNOWLEDGMENTS

We thank H.-J. Queisser for his support throughout this work. The excellent technical assistance of W. Heinz and W. Krause is acknowledged.

*Permanent address: School of Physical Sciences, Jawaharlal Nehru University, New Delhi 110067, India.

[†]Present address: TU Dresden, Institut für Tieftemperaturphysik, D-01062 Dresden, Germany.

¹For a recent review, see *Germanium Silicon: Physics and Materials*, edited by R. Hull and J.C. Bean (Academic Press, Boston, 1999), Vol. 56.

²T.P. Pearsall, J.M. Vandenberg, R. Hull, and J.M. Bonar, *Phys. Rev. Lett.* **63**, 2104 (1989).

³R. Zachai, K. Eberl, G. Abstreiter, E. Kasper, and H. Kibbel, *Phys. Rev. Lett.* **64**, 1055 (1990).

⁴U. Menczgar, G. Abstreiter, J. Olajos, H. Grimmeiss, H. Kibbel, H. Presting, and E. Kasper, *Phys. Rev. B* **47**, 4099 (1993).

⁵T.P. Pearsall, H. Polatoglou, H. Presting, and E. Kasper, *Phys. Rev. B* **54**, 1545 (1996).

⁶U. Gnutzmann and K. Clausecker, *Appl. Phys.* **3**, 9 (1974).

⁷R.J. Turton and M.J. Jaros, *Mater. Sci. Eng.*, **B 7**, 37 (1990).

⁸S. Satpathy, R.M. Martin, and C.G. Van de Walle, *Phys. Rev. B* **38**, 13 237 (1988).

⁹I. Morrison and M. Jaros, *Phys. Rev. B* **37**, 916 (1988).

¹⁰C. Tserbak, H.M. Polatoglou, and G. Theodorou, *Phys. Rev. B* **47**, 7104 (1993).

¹¹U. Schmid, N.E. Christensen, and M. Cardona, *Phys. Rev. Lett.*

65, 2610 (1990).

¹²J.P. Noel, N.L. Rowell, D.C. Houghton, and D.D. Perovic, *Appl. Phys. Lett.* **57**, 1037 (1990).

¹³J. Weber and M.I. Alonso, *Phys. Rev. B* **40**, 5683 (1989).

¹⁴S.T. Lai and M.V. Klein, *Phys. Rev. Lett.* **44**, 1087 (1980); *Phys. Rev. B* **29**, 3217 (1984).

¹⁵M. Oueslati, M. Zouaghi, M.E. Pistol, L. Samuelson, H.G. Grimmeiss, and M. Balkanski, *Phys. Rev. B* **32**, 8220 (1985).

¹⁶L.C. Lenchyshyn, M.L.W. Thewalt, J.C. Sturm, P.V. Schwartz, E.J. Prinz, N.L. Powell, J.P. Noel, and D.C. Houghton, *Appl. Phys. Lett.* **60**, 3174 (1992).

¹⁷L.C. Lenchyshyn, M.L.W. Thewalt, D.C. Houghton, J.P. Noel, N.L. Rowell, J.C. Sturm, and X. Xiao, *Phys. Rev. B* **47**, 16 655 (1993).

¹⁸R. Schorer, E. Friess, K. Eberl, and G. Abstreiter, *Phys. Rev. B* **44**, 1772 (1991).

¹⁹W. Ge, M.D. Sturge, W.D. Schmidt, L.N. Pfeiffer, and K.W. West, *Appl. Phys. Lett.* **57**, 55 (1990); D.G. Thomas, *Phys. Rev. Lett.* **17**, 1262 (1966).

²⁰N.N. Ledentsov, J. Bohrer, M. Beer, F. Heinrichsdorff, M. Grundmann, D. Bimberg, S.V. Ivanov, B.Ya. Meltser, S.V. Shaposhnikov, I.N. Yassievich, N.N. Faleev, P.S. Kopev, and Zh.I. Alferov, *Phys. Rev. B* **52**, 14 058 (1995).